Active coupled-resonator optical waveguides. I. Gain enhancement and noise

Joyce K. S. Poon* and Amnon Yariv

Department of Electrical Engineering, California Institute of Technology, MS 136-93, Pasadena, California 91125, USA
**Corresponding author: poon@caltech.edu*

Received May 10, 2007; accepted June 4, 2007;
posted July 5, 2007 (Doc. ID 82868); published August 24, 2007

We use a tight-binding formalism in the time domain to analyze the effect of resonant gain enhancement and spontaneous emission noise in amplifying coupled-resonator optical waveguides (CROWs). We find the net amplification of a wave propagating in a CROW does not always vary with the group velocity, and depends strongly on the termination and excitation of these structures. The signal-to-noise ratio and noise figure of CROW amplifiers are derived in the tight-binding formalism as well. The physical interpretations and practical consequences of the theoretical results are discussed. © 2007 Optical Society of America

OCIS codes: 230.5750, 250.4480, 140.3290.

1. INTRODUCTION

A coupled-resonator optical waveguide (CROW) is a periodic array of resonators in which light propagates due to the weak coupling between its nearest neighbors [1,2]. An interesting property of CROWs is that light can propagate at a significantly reduced group velocity, dictated by the interresonator coupling, with no group velocity dispersion at the band-center [3]. As fabrication technologies improve, very high-order, even on the order of a hundred, coupled resonators are now achievable [4–9].

One of the important challenges that remains is to overcome the optical loss in these structures. Intuitively, the loss accumulated in these devices can scale with the number of resonators in the structures and the time delay [10] (we shall show in this paper that this is not always the case). Therefore, to compensate for the accumulated losses, an amplifying section that is placed after a CROW may have to be long, perhaps much longer than the CROW itself. Thus, to avoid additional device footprint, it would be advantageous to continuously amplify a wave propagating in an active CROW.

In this paper and the companion paper [11], we shall investigate theoretically and experimentally active, amplifying CROWs. This paper will examine theoretically the effect of resonant gain enhancement and noise. Using a tight-binding analysis, we will show that for real values of the coupling constant, the net gain of a wave in a finite-length CROW does not necessarily depend only on its group velocity, but is also strongly affected by the excitation and termination of the CROW. These results can be applied to losses as well, though optical gain makes laser oscillation possible and must be considered with more care. Using the same formalism, we will find the expression for the noise caused by spontaneous emission. The measurements of amplifying CROWs in the form of InP–InGaAsP Fabry–Perot resonator arrays are discussed in [11].

2. TIME DOMAIN TIGHT-BINDING EQUATIONS

To provide a generalized approach to analyze the amplifying and noise properties of CROWs, we shall use a time domain tight-binding or coupled-mode formalism. Time domain coupled-mode equations are commonly used to analyze coupled resonators [12–14]. In this section, we shall outline the derivation of these time domain coupled-mode or tight-binding equations from Maxwell's equations. The derivation will make the assumptions that are made in obtaining the simple coupled oscillator equations found in the literature explicit [12–14].

To analyze gain/loss as well as noise, we first define the polarization density of the structure as

$$\mathbf{P}(\mathbf{r},t) = \epsilon_0 \chi(\mathbf{r})\mathbf{E} + \epsilon_0 \mathbf{p}(\mathbf{r},t), \tag{1}$$

where $\chi(\mathbf{r})$ is the susceptibility and $\mathbf{p}(\mathbf{r},t)$ is the small amplitude fluctuation of $\mathbf{P}(\mathbf{r},t)$ which we will use later in our analysis of noise. Generally speaking, in active structures, the susceptibility is a function of time, since the carrier or population densities are modified by the optical field. We shall simplify the analysis to a quasi-static picture where the optical signal varies on a much longer time scale than the carrier dynamics, so that the gain and loss can be taken as constants. Furthermore, in the regime of small values of gain, we can neglect nonlinearities due to saturation so that $\chi(\mathbf{r})$ is linear and can be expressed as $\chi(\mathbf{r}) = \epsilon(\mathbf{r}) + i\sigma(\mathbf{r})$. The variable $\epsilon(\mathbf{r})$ is the dielectric profile of the structure, and $\sigma(\mathbf{r})$ accounts for the gain or loss depending on its sign (positive for gain and negative for loss). Substituting the polarization density into Maxwell's equations, we arrive at

$$\nabla \times \nabla \times \mathbf{E}(\mathbf{r},t) + \frac{1}{c^2}[\epsilon(\mathbf{r}) + i\sigma(\mathbf{r})]\ddot{\mathbf{E}}(\mathbf{r},t) = -\frac{1}{c^2}\ddot{\mathbf{p}}(\mathbf{r},t). \tag{2}$$

In the tight-binding or coupled-mode approach, we assume that the fields in a CROW, $\mathbf{E}(\mathbf{r},t)$, can be expressed as a superposition of the localized resonator modes, $\mathbf{E}_\Omega(\mathbf{r})$. Strictly speaking, in the presence of loss or gain, the structure does not support true eigenmodes [15,16]. However, we shall assume that the index contrast is sufficiently high and the loss/gain small, so that these "quasimodes" are well approximated by an expansion over the lossless resonator modes. Therefore, for a CROW consisting of N identical resonators, the field is

$$\mathbf{E}(\mathbf{r},t) = \exp(i\omega t)\sum_{n=1}^{N} a_n(t)\mathbf{E}_\Omega(\mathbf{r} - n\Lambda\hat{z}), \tag{3}$$

where $a_n(t)$ is a time-dependent amplitude coefficient, $\hat{z}$ is the direction of periodicity, and Λ is the period. $a(t)$ varies slowly compared to the optical frequency. We note that the localized resonator modes themselves satisfy the equation

$$\nabla \times \nabla \times \mathbf{E}_\Omega(\mathbf{r}) = \frac{\Omega^2}{c^2}\epsilon_\Omega(\mathbf{r})\mathbf{E}_\Omega(\mathbf{r}), \tag{4}$$

where Ω is the resonance frequency and $\epsilon_\Omega(\mathbf{r})$ is the dielectric constant of the single resonator.

Substituting Eqs. (3) and (4) into Eq. (2), and applying the slowly varying envelope approximation, $|\ddot{a}_n| \ll 2\omega|\dot{a}_n|$, we drop the $\ddot{a}_n$ terms. The slowly varying envelope approximation is valid only in the case of weak interresonator coupling, meaning that

$$\int \mathrm{d}^3\mathbf{r}\mathbf{E}_\Omega^*(\mathbf{r} - \Lambda\hat{z})f(\mathbf{r})\mathbf{E}_\Omega(\mathbf{r}) \ll \int \mathrm{d}^3\mathbf{r}\mathbf{E}_\Omega^*(\mathbf{r})f(\mathbf{r})\mathbf{E}_\Omega(\mathbf{r}), \tag{5}$$

where $f(\mathbf{r}) = \epsilon(\mathbf{r})$ or $|\sigma(\mathbf{r})|$. Typically, $|\sigma(\mathbf{r})|$ is much smaller than $\epsilon(\mathbf{r})$. However, at certain material resonances, the imaginary part of the susceptibility can dominate so that the resonators can be coupled through $\sigma(\mathbf{r})$ as well.

Subsequently, we integrate the result over $\int \mathrm{d}^3\mathbf{r}\mathbf{E}_\Omega^*(\mathbf{r} - m\Lambda\hat{z})$, and keep only up to nearest neighbor interaction terms (i.e., only the $n=m$, $m\pm1$ terms). We further approximate that the $\dot{a}_{m\pm1}$ terms are negligible compared to the $\dot{a}_m$ term, which is again only valid in the weak coupling regime. To simplify the expressions, we may adopt the normalization condition $\int \mathrm{d}^3\mathbf{r}\mathbf{E}_\Omega^*(\mathbf{r})\cdot\epsilon_\Omega(\mathbf{r})\mathbf{E}_\Omega(\mathbf{r}) = 1$. At this point, we arrive at

$$\begin{aligned} 2i\omega\dot{a}_m(1 + \Delta\alpha + i\sigma_m) = {} & a_m[(\omega^2 - \Omega^2) + \omega^2(\Delta\alpha + i\sigma_m)] \\ & + a_{m+1}[\omega^2(d + i\Delta\sigma) - \Omega^2 b] \\ & + a_{m-1}[\omega^2(d^* + i\Delta\sigma^*) - \Omega^2 b^*] \\ & - \ddot{p}_m \exp(-i\omega t), \end{aligned} \tag{6}$$

where the various constants are given by

$$\Delta\alpha = \int \mathrm{d}^3\mathbf{r}\mathbf{E}_\Omega^*(\mathbf{r})\cdot[\epsilon(\mathbf{r}) - \epsilon_\Omega(\mathbf{r})]\mathbf{E}_\Omega(\mathbf{r}), \tag{7a}$$

$$b = \int \mathrm{d}^3\mathbf{r}\mathbf{E}_\Omega^*(\mathbf{r})\cdot\epsilon_\Omega(\mathbf{r} - \Lambda\hat{z})\mathbf{E}_\Omega(\mathbf{r} - \Lambda\hat{z}), \tag{7b}$$

$$d = \int \mathrm{d}^3\mathbf{r}\mathbf{E}_\Omega^*(\mathbf{r})\cdot\epsilon(\mathbf{r})\mathbf{E}_\Omega(\mathbf{r} - \Lambda\hat{z}), \tag{7c}$$

$$\sigma_m = \int \mathrm{d}^3\mathbf{r}\mathbf{E}_\Omega^*(\mathbf{r})\cdot\sigma(\mathbf{r})\mathbf{E}_\Omega(\mathbf{r}), \tag{7d}$$

$$\Delta\sigma_m = \int \mathrm{d}^3\mathbf{r}\mathbf{E}_\Omega^*(\mathbf{r})\cdot\sigma(\mathbf{r})\mathbf{E}_\Omega(\mathbf{r} - \Lambda\hat{z}), \tag{7e}$$

$$p_m = \int \mathrm{d}^3\mathbf{r}\mathbf{E}_\Omega^*(\mathbf{r} - m\Lambda\hat{z})\cdot\mathbf{p}(\mathbf{r}). \tag{7f}$$

To simplify the algebra, we have assumed that $\epsilon(\mathbf{r}) \approx \epsilon(\mathbf{r}\pm\Lambda\hat{z})$, which is true only for infinitely long structures. The approximation holds the worst for the first and last resonators in a finite CROW. This means that the constants in Eq. (7) at the first and last resonators are slightly different compared to resonators in the center of the chain.

If $\Delta\alpha$, $|\sigma_m| \ll 1$, and $\omega \approx \Omega$, such that both the gain and the coupling are weak, Eq. (6) becomes

$$\begin{aligned} i\dot{a}_m = {} & a_m\left[(\omega - \Omega') + i\frac{\omega\sigma_m}{2}\right] + \kappa a_{m+1} + \kappa^* a_{m-1} \\ & - \frac{\ddot{p}_m}{2\omega}\exp(-i\omega t), \end{aligned} \tag{8}$$

where $\Omega' = \Omega - \omega\Delta\alpha/2$, and $\kappa = \omega/2(d - b)$, or

$$\kappa = \frac{\omega}{2}\int \mathrm{d}^3\mathbf{r}\mathbf{E}_\Omega^*(\mathbf{r})[\epsilon(\mathbf{r} + m\Lambda\hat{z}) - \epsilon_\Omega(\mathbf{r} - \Lambda\hat{z})]\mathbf{E}_\Omega(\mathbf{r} - \Lambda\hat{z}). \tag{9}$$

In reaching Eq. (8), we neglected terms that vary with $\Delta\sigma_m$ by assuming that the coupling through the real part of the susceptibility dominates. However, in the case where $\Delta\sigma_m$ cannot be neglected, the coupling constant will be a complex number with an imaginary part given by $i\omega\Delta\sigma_m/2$.

Because a CROW consisting of weakly coupled resonators is a narrowband device, if we consider only the noise in the frequency range of a single propagation band, the noise term, $p_m(t)$ can be approximated as a slowly varying complex amplitude, so it can be expressed as $p_m(t) = 2s_m(t)\exp(i\omega t)$ and $\ddot{p}_m \approx -2\omega^2 s_m(t)\exp(i\omega t)$. With this final approximation, and choosing the phase such that $\mathbf{E}_\Omega$ is real and $\kappa = \kappa^*$, we finally arrive at the typical time domain coupled oscillator equation,

$$\dot{a}_m = a_m\left[-i(\omega - \Omega') + \frac{1}{\tau_i}\right] - i\kappa(a_{m+1} + a_{m-1}) - i\omega s_m(t), \tag{10}$$

where we have defined $1/\tau_i \equiv \omega\sigma_m/2$. The equation $\tau_i > 0$ represents gain, while $\tau_i < 0$ represents loss.

Throughout our derivation, we have highlighted the approximations that are embodied by Eq. (10). These ap-

proximations are justified in the regime of weak interresonator coupling and small values of gain or loss. In the limit of high gain or high field intensities, light propagation becomes nonlinear because of saturation. To deal with large coupling strengths, transfer matrices are an alternative analytical approach [17,18].

3. GAIN ENHANCEMENT AND BOUNDARY CONDITIONS

In this section, we will use the coupled oscillator equation, Eq. (10), derived in Section 2 to understand the role of coupled resonances on the net gain of an amplifying CROW. We shall neglect the noise contribution here and examine the steady-state response, so that $s_m(t)=0$ and $\dot{a}_m=0$ in Eq. (10). Our results will show that gain enhancement is strongly dependent on the boundary conditions and the excitation of the coupled resonators. We will examine the following several scenarios illustrated in Fig. 1: (a) infinite structures, (b) finite structures in isolation of additional dissipative pathways, (c) finite structures with additional dissipation (such as input/output waveguides), and (d) finite structures driven by input optical fields.

A. Infinitely Long Structures

An infinitely long CROW is schematically depicted in Fig. 1(a). The eigenmodes of infinitely long structures satisfy Bloch boundary conditions so that $a_{m+1}=a_m \exp(-iK\Lambda)$, where K is the Bloch wave vector. K can be complex and can be expressed as $K=K_R+iK_I$. Substituting this form of the solution into Eq. (10), we have the following equations for the real and imaginary parts of Eq. (10):

$$(\omega-\Omega')=-2\kappa\cos(K_R\Lambda)\cosh(K_I\Lambda), \tag{11a}$$

$$-\frac{1}{\tau_i}+2\kappa\sin(K_R\Lambda)\sinh(K_I\Lambda)=0. \tag{11b}$$

In the absence of loss or gain, $K_I=0$, thus the group velocity of a lossless and nonamplifying structure, $\bar{v}_g$, is $d\omega/dK=2\kappa\Lambda\sin(K_R\Lambda)$. However, in general, the band-structure and, hence the group velocity, can be modified by gain and loss [19]. Substituting $\bar{v}_g$ into Eq. (11b) gives

$$\sinh(K_I\Lambda)=\frac{\Lambda}{2\tau_i\bar{v}_g}. \tag{12}$$

As $\bar{v}_g\to 0$, $K_I\to\infty$, meaning that the field is most amplified (or attenuated) at the band-edges. For small values of $K_I\Lambda$, near the band-center, $K_I\Lambda\approx\Lambda/2\tau_i\bar{v}_g$ and scales linearly with $\bar{v}_g$. Therefore, for infinitely long structures, the gain (loss) of the Bloch modes of the coupled resonators are enhanced compared to the gain (or loss) of the constituent resonators by a factor of $1/\bar{v}_g$. This result agrees well with conventional arguments in describing band-edge laser action and gain enhancement in photonic crystals where the analysis often begins with the Bloch modes of the structures [20–22].

B. Finite Structures

Naturally, infinitely long structures are not realizable in practice. In this subsection, we shall show that even if the finite structures contain a very large number of periods, the modes can behave significantly different compared to the Bloch modes. In particular, the termination or boundary conditions play perhaps the most important role in determining the net gain (loss) in the coupled resonator chains.

The field amplitudes in finite structures can be solved by expressing Eq. (10) in terms of a matrix equation. For convenience, we define $\mathbf{a}\equiv[a_1\ a_2\ \cdots\ a_N]^T$. In the following sections, we shall find the fields of finite CROWs with various boundary conditions.

1. Clamped Boundaries

First, we examine the modes of a finite CROW with no external coupling to dissipation channels, in addition to the intrinsic gain/loss rate of $1/\tau_i$. This situation is depicted in Fig. 1(b). In this scenario, because of the finite length of the CROW, the fields are "clamped" to zero at the boundaries, or $a_0=0$ and $a_{N+1}=0$. The matrix equation that describes this system is

$$i\omega\mathbf{a}=\begin{bmatrix} i\Omega'+\frac{1}{\tau_i} & -i\kappa & 0 & 0 & \cdots & 0 & 0 \\ -i\kappa & i\Omega'+\frac{1}{\tau_i} & -i\kappa & 0 & \cdots & 0 & 0 \\ . & . & . & . & . & . & . \\ . & . & . & . & . & . & . \\ . & . & . & . & . & -i\kappa & i\Omega'+\frac{1}{\tau_i} \end{bmatrix}\mathbf{a}. \tag{13}$$

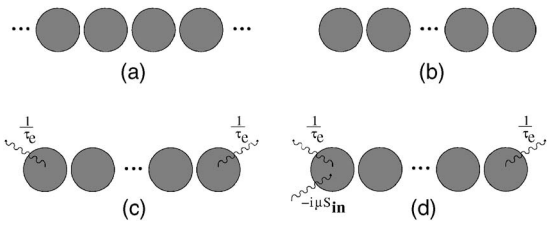

Fig. 1. Various configurations of coupled resonators: (a) infinitely long CROWs, (b) finite CROWs in isolation, (c) finite CROWs with out-coupling at the ends, and (d) finite CROWs with an input optical field with out-coupling at the ends.

The eigenvalues, ω_n, and the elements of the eigenvectors, $\mathbf{a}_m$, of Eq. (13) are [23]

$$\omega_n = \left(\Omega' - \frac{i}{\tau_i}\right) - 2\kappa\cos\left(\frac{n\pi}{N+1}\right), \quad n = 1\cdots N, \tag{14a}$$

$$\mathbf{a}_m = \sin\left(m\frac{n\pi}{N+1}\right), \quad m = 1\cdots N. \tag{14b}$$

From Eq. (14a), the real part of ω_n gives the dispersion relation of the structure as $N\to\infty$. However, the imaginary part of all the eigenvalues are identical and equal $-i/\tau_i$, independent of $n\pi/(N+1)$. Therefore, regardless of how many resonators are in the chain, all of the modes experience equal amplification and dissipation rates. Unlike the Bloch modes in Section 3.A, there is no additional enhancement of the gain loss that arises from the coupling between the resonators compared to the intrinsic gain loss of the individual resonators. Physically, this result is not surprising because these boundary conditions imply that the standing-wave modes of the finite CROW are isolated from the external world, so that the fields of the CROW grow (or decay) at the same rate as its constituent resonators.

2. Free Boundaries

Next, we shall allow for additional dissipation in the CROW. Most typically, this corresponds to the scenario where light is coupled out somewhere in the CROW via waveguides for example. We will now examine the specific case where this out-coupling occurs at the first and last elements in the CROW as we show in Fig. 1(c), though our approach can easily be generalized to outcoupling at other elements. Because we shall allow for additional dissipation at the ends of the CROW, the fields are no longer clamped at the boundaries and are "free."

For these boundary conditions, we can express the fields as

$$i\omega\mathbf{a} = \begin{bmatrix} i\Omega' + \frac{1}{\tau_i} - \frac{1}{\tau_e} & -i\kappa & 0 & 0 & \cdots & 0 & 0 \\ -i\kappa & i\Omega' + \frac{1}{\tau_i} & -i\kappa & 0 & \cdots & 0 & 0 \\ . & . & . & . & . & . & . \\ . & . & . & . & . & . & . \\ . & . & . & . & . & -i\kappa & i\Omega' + \frac{1}{\tau_i} - \frac{1}{\tau_e} \end{bmatrix}\mathbf{a}, \tag{15}$$

where $1/\tau_e > 0$ is the additional loss rate to the external world. In general, the eigenvalues of Eq. (15) are found numerically. However, we can readily find an explicit analytical expression using our results from Eq. (14) if $1/\tau_e$ can be accounted for perturbatively.

Perturbatively, the first-order correction to Eq. (14a) due to $1/\tau_e$ is given by $\mathbf{a}_n^T W \mathbf{a}_n$, where $\mathbf{a}_n$ is the normalized eigenvector and W is the perturbation. The resultant eigenvalues are

$$\omega_n = \Omega' + 2\kappa\cos\left(\frac{n\pi}{N+1}\right) + i\left[-\frac{1}{\tau_i} + \frac{2}{\tau_e}\frac{\sin^2(n\pi/N+1)}{\sum_{m=1}^{N}\sin^2(m(n\pi/N+1))}\right]. \tag{16}$$

Equation (16) shows that $1/\tau_i$ again does not scale with $n/(N+1)$, thus there is no gain enhancement that depends on $1/\bar{v}_g$. However, the rate of amplification is indeed higher at the band-edges ($n\approx 0, N$) compared to the band-center, because for $\tau_i > 0$, the imaginary part of ω_n is more negative at the band-edges compared to the band-center. Nonetheless, this increased gain at the band-edges is wholly determined by the external coupling.

Figure 2 illustrates this result, where we have the numerically computed eigenvalues of Eq. (15), and the eigenvalues described by Eq. (16) for the parameters described in the caption. The parameters are normalized to Ω'. The rate of amplification is given by $-\mathrm{Im}[\omega_n]$ and is plotted against $\mathrm{Re}[\omega_n]-\Omega'$. As it is evidenced by the figure, the frequencies near the band-edge experience an increased rate of amplification proportional to the out-coupling rate.

Physically, we can interpret the $1/\tau_e$ term in Eq. (16) as the effective rates of dissipation or out-coupling of the various CROW modes described by Eq. (14). This effective rate is smallest at the band-edges and largest at the band-center as though the termination is lower loss (more "reflective") for the lower $\bar{v}_g$ modes [24].

3. Forced Coupled Oscillators

Thus far, we have only examined eigenmodes of infinite and finite CROWs. The eigenmodes are useful when an input optical wave indeed excites superpositions of these modes. In this section, we examine the transmission of a CROW amplifier where the first resonator is excited by an input wave, and the output is detected at the last resonator as in Fig. 1(d).

To model the presence of an input source, we add a driving term to the first resonator, $-i\mu S_{in}$, where μ describes the strength of the coupling between the input wave and the resonator. Thus, the matrix equation becomes

$$i\omega\mathbf{a} = \begin{bmatrix} i\Omega' + \frac{1}{\tau_i} - \frac{1}{\tau_e} & -i\kappa & 0 & 0 & \cdots & 0 & 0 \\ -i\kappa & i\Omega' + \frac{1}{\tau_i} & -i\kappa & 0 & \cdots & 0 & 0 \\ \cdot & \cdot & \cdot & \cdot & \cdot & \cdot & \cdot \\ \cdot & \cdot & \cdot & \cdot & \cdot & \cdot & \cdot \\ \cdot & \cdot & \cdot & \cdot & \cdot & -i\kappa & i\Omega' + \frac{1}{\tau_i} - \frac{1}{\tau_e} \end{bmatrix} \mathbf{a} - i\mu \begin{bmatrix} S_{in} \\ 0 \\ \cdot \\ \cdot \\ 0 \end{bmatrix} \equiv \mathsf{M}\mathbf{a} - i\mu\mathbf{s}_{in}. \tag{17}$$

Therefore, the amplitudes in the resonators are given by

$$\mathbf{a} = -i\mu(i\omega\mathsf{I} - \mathsf{M})^{-1}\mathbf{s}_{in} \equiv -i\mu\mathsf{T}\mathbf{s}_{in}. \tag{18}$$

The transmitted amplitude, S_t, is proportional to the amplitude in the last resonator, which is given by $a_N = -i\mu\mathsf{T}_{N,1}S_{in}$.

The constant of proportionality between S_t and a_N is determined from the conservation of energy in the absence of gain and loss. For example, we can consider a single resonator where the rates of out-coupling to the input and output waveguides are identical. If the magnitude of the field amplitude at the output is equal to the input on resonance then, from Eq. (10),

$$-\frac{2}{\tau_e}a_1 - i\mu S_{in} = 0. \tag{19}$$

The factor of 2 is due to out-coupling to both input and output waveguides. If $|S_t|^2 = |S_{in}|^2$, as in the case of ring resonators in the add-drop configuration [13], then $|S_t|^2 = |2/(\tau_e\mu)a_1|^2$ and $|\bar{\kappa}| = |2/(\tau_e\mu)|$ is the fraction of field amplitude inside the resonator leaked out to the output waveguide. For standing-wave resonators, $|S_t|^2$ is divided into four output channels (two at the start of the CROW and two at the end) [18]. Therefore, generalizing to a CROW using Eq. (18), the transmitted amplitude is

$$\left|\frac{S_t}{S_{in}}\right|^2 = \left|\frac{2}{\tau_e}\mathsf{T}_{N,1}\right|^2. \tag{20}$$

The matrix element, $\mathsf{T}_{N,1}$, is explicitly given by [25]

$$\mathsf{T}_{N,1} = \frac{\kappa \sin(\phi)}{i/\tau_e^2 \sin((N-1)\phi) + 2\kappa/\tau_e \sin(N\phi) - i\kappa^2 \sin((N+1)\phi)}, \tag{21a}$$

$$\cos(\phi) = -\frac{(\omega - \Omega')}{2\kappa} - \frac{i}{2\kappa\tau_i}, \tag{21b}$$

for $\tau_i \neq 0$. At the band edges, $\cos(\phi_{be}) = \pm 1 - i/(2\kappa\tau_i)$, and at the band-center, $\cos(\phi_{bc}) = -i/(2\kappa\tau_i)$. This equation can be solved numerically. However, from Eqs. (20) and (21), we see that the transmitted amplitude depends solely on $\kappa\tau_e$ at a fixed ϕ. Thus, the net gain or loss experienced by the transmitted field can be changed via τ_e.

Figure 3 shows the numerically calculated transmission amplitude using Eq. (21) for various values of $1/\tau_e$.

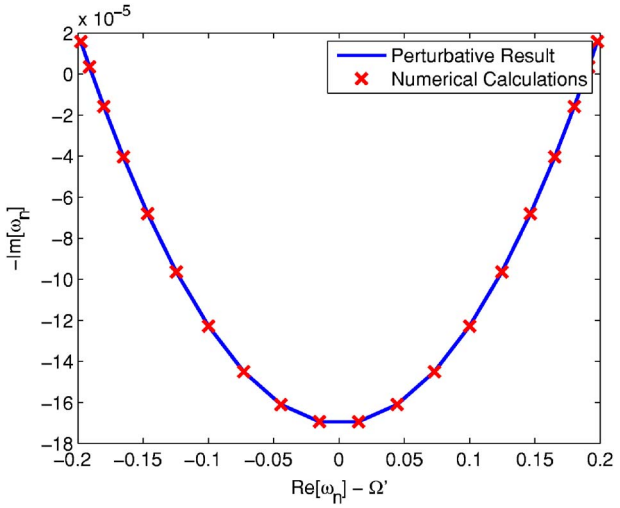

Fig. 2. (Color online) $-\mathrm{Im}[\omega_n]$ versus $\mathrm{Re}[\omega_n]-\Omega'$ for the CROW with out-coupling at two ends. $\tau_e = 10^4$, $\tau_i = 5\times10^4$, $\kappa = 0.1$, and $N = 20$.

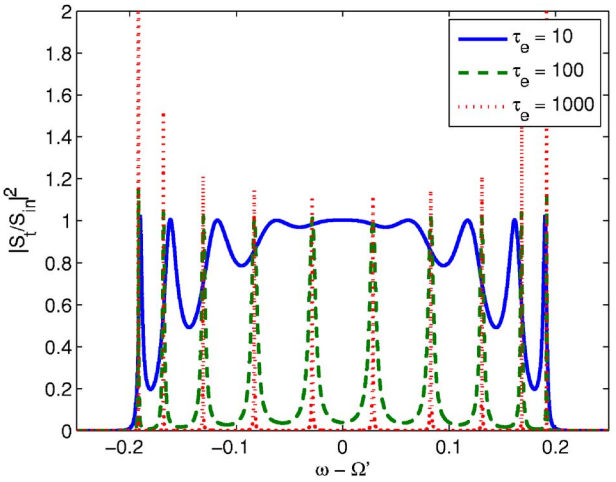

Fig. 3. (Color online) The transmittance, $|S_t/S_{in}|^2$, of CROWs for various values of τ_e. The other parameters are $\tau_i=5\times10^4$, $\kappa=0.1$, and $N=10$. Only the portion of $|S_t/S_{in}|^2\leq2$ is shown for comparison.

The other parameters for the calculations are described in the figure caption. As evidenced by the plot, the net gain of a wave and its transmittance is controlled by τ_e. Naturally, the loss and gain through a finite CROW can also be controlled by τ_i for a fixed τ_e [26].

Although Eq. (21) should in general be solved numerically, we can easily find some approximate results in the case of loss, $\tau_i<0$, for which the equation does not possess any poles. In the regime where $1/(\kappa|\tau_i|)\ll1$ and $N/(2\kappa|\tau_i|)\gg1$, after some algebra, the transmitted amplitude at the band-center is approximately given by

$$\left|\frac{S_t}{S_{in}}\right|_{bc}\approx\frac{4e^{\frac{N}{2\kappa\tau_i}}}{1/(\kappa\tau_e)+2+\kappa\tau_e}\quad\tau_i<0. \tag{22}$$

Equation (22) gives the transmittance with loss and is in agreement with the heuristic argument presented in Ref. [10] when $\kappa\approx1/\tau_e$. Figure 4 shows the transmittance as a function of the number of resonators at the band-center frequency, $\omega=\Omega'$, computed using Eqs. (21) and (22). The plot shows that Eq. (22) is an excellent approximation to Eqs. (21).

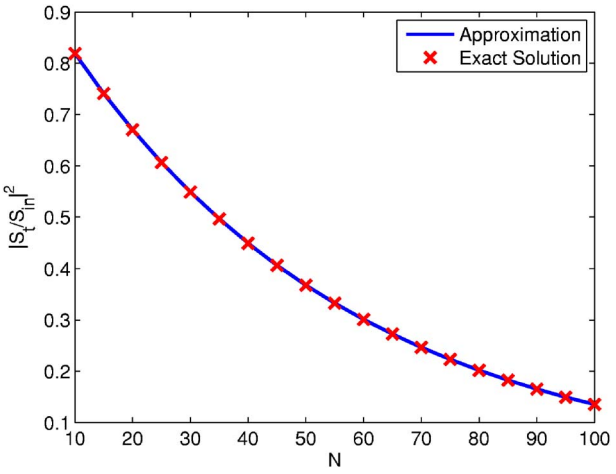

Fig. 4. (Color online) The exact solution of the transmittance from Eq. (21) and the approximation given by Eq. (22) as a function of the number of resonators (N) at the band-center frequency with optical loss. The other parameters are $\tau_i=-5\times10^3$, $\kappa=0.01$, $\tau_e=1/\kappa=100$.

4. SPONTANEOUS EMISSION NOISE

In optically amplifying devices, the effect of noise from the spontaneous emission, which can obscure the signal is as important as the magnitude of the transmission. Using the formalism we developed in Section 2, we can explicitly examine the effect of spontaneous emission in a CROW. We will make frequent use of the Fourier transform in this section, which we define as

$$f(t)=\int_{-\infty}^{\infty}\tilde{f}(\tilde{\omega})\exp(i\tilde{\omega}t)\mathrm{d}\tilde{\omega}, \tag{23a}$$

$$\tilde{f}(\tilde{\omega})=\frac{1}{2\pi}\int_{-\infty}^{\infty}f(t)\exp(-i\tilde{\omega}t)\mathrm{d}t. \tag{23b}$$

We begin in the tight-binding picture with Eq. (10). Spontaneous emission causes small fluctuations in the polarization density in the medium, and is the basis of $s_m(t)$. From Eq. (10), we can see that the spontaneous emission is manifested as a small amplitude input at each resonator, which can then propagate and be amplified in the CROW. A simple way to analyze the noise is to work in the frequency domain so that we will have a linear set of equations. Taking the Fourier transform of Eq. (10), we have

$$i\tilde{\omega}\tilde{a}_m=\tilde{a}_m\left[-i\Delta+\frac{1}{\tau_i}\right]-i\kappa(\tilde{a}_{m+1}+\tilde{a}_{m-1})-i\omega\tilde{s}_m, \tag{24}$$

where $\tilde{a}_m$, $\tilde{a}_{m\pm1}$, $\tilde{s}_m$ are the Fourier amplitudes of a_m, s_m, and $a_{m\pm1}$ respectively, $\tilde{\omega}$ is a frequency that is much lower than the optical frequency, and $\Delta\equiv\omega-\Omega'$. Equation (24) can now be solved as a matrix equation to find $\tilde{a}_m$ provided that $\tilde{s}_m$ is known.

A. Normalization of $\tilde{s}_m(\tilde{\omega})$

The normalization of $\tilde{s}_m$ is related to the amount of spontaneous emission. We can readily determine $\tilde{s}_m$ of each resonator by assuming there is no additional input wave, and taking $\kappa=0$. For clarity, we separate the contributions of the gain/absorption (due to induced transitions) and the intrinsic loss of the resonator:

$$1/\tau_i=1/\tau_g-1/\tau_l, \tag{25}$$

where $1/\tau_g$ gives the amplification/absorption rate of the active medium, and $1/\tau_l$ is the intrinsic loss rate. The fraction $1/\tau_g$ depends on the inversion of the material and can be negative or positive depending on the pumping. The fraction $1/\tau_l$ is a positive quantity.

At the material transparency, $1/\tau_g=0$, the spontaneously emitted wave, $\tilde{a}_{sp}$, at the resonant frequency is

$$i\tilde{\omega}\tilde{a}_{sp,m} = -\frac{1}{\tau_l}\tilde{a}_{sp,m} - i\Omega\tilde{s}_m, \tag{26}$$

and its magnitude is

$$|\tilde{a}_{sp,m}|^2 = \frac{\Omega^2}{\tilde{\omega}^2 + 1/\tau_l^2}|\tilde{s}_m|^2. \tag{27}$$

The instantaneous energy of the spontaneous emission is

$$U_{sp,m}(t) = |a_{sp,m}(t)|^2 \int \mathrm{d}^3\mathbf{r}\epsilon_0\epsilon_\Omega(\mathbf{r})|E_\Omega(\mathbf{r})|^2 = |a_{sp,m}(t)|^2 V, \tag{28}$$

where $V \equiv \epsilon_0 \int d^3\mathbf{r}\epsilon_\Omega(\mathbf{r})|E_\Omega(\mathbf{r})|^2$. Therefore, from the Weiner–Khintchine theorem, the average energy is

$$\langle U_{sp,m}\rangle = \lim_{T\to\infty}\frac{1}{T}\int_{-T/2}^{T/2}\mathrm{d}t U_{sp,m}(t)$$

$$= \lim_{T\to\infty}\frac{2\pi V}{T}\int \mathrm{d}\tilde{\omega}|\tilde{a}_{sp,m}(\tilde{\omega})|^2, \tag{29}$$

where T is interpreted as the measurement integration time [23]. However, the spontaneous emission power into an ideal single uncoupled resonator is $P_{sp,m}\approx R_{sp,m}\hbar\Omega$, where $R_{sp,m}$ is the rate of spontaneous emission. $R_{sp,m}$ is a function of the pump rate and can be modified compared to bulk dielectrics by the Purcell factor [15]. As the coupling to its neighbors increases, $R_{sp,m}$ of a single cavity will be modified. For simplicity, let us assume that the resonators are sufficiently weakly coupled so that $R_{sp,m}$ does not change appreciably in the coupled resonator chain. Since the spontaneous emission dissipates from the resonator at a rate of $2/\tau_l$,

$$\langle U_{sp,m}\rangle = \frac{P_{sp,m}\tau_l}{2} = \frac{R_{sp,m}\hbar\Omega\tau_l}{2}. \tag{30}$$

Therefore, using Eqs. (27), (29), and (30), as $1/\tau_l\to 0$ (i.e., small values of intrinsic loss), we arrive at the normalization condition,

$$\lim_{T\to\infty}\frac{|\tilde{s}_m(0)|^2}{T} = \frac{\hbar R_{sp,m}}{4\pi^2 V\Omega}, \tag{31}$$

where we have used the identity $\lim_{\epsilon\to 0}\epsilon/(x^2+\epsilon^2)=\pi\delta(x)$. It is important to note that $R_{sp,m}$, τ_l, and τ_g are not independent of each other, and are related through the cavity losses and the carrier densities. In Subsection 4.B, we will use the result in Eq. (31) to derive the signal-to-noise ratio in active CROWs.

B. Signal-to-Noise Ratio

An important metric of propagating optical signals in any amplifying structure with gain is the signal-to-noise ratio (SNR). SNRs in nonresonant and Fabry–Perot amplifiers, as well as noise in multielement lasers have been studied [16,23,27–29]. Here, we use our tight-binding formalism to derive expressions for the SNR of a CROW amplifier. In particular, we will focus on the case described in Subsection 3.B.3 where the CROW is excited by an input wave at the first resonator, and the signal is detected at the output at the last resonator. Our approach can be easily extended to other excitation conditions and boundary conditions.

We begin with the matrix form of Eq. (24) with an input in the first resonator, so that

$$\begin{bmatrix} -i(\tilde{\omega}+\Delta)+\frac{1}{\tau_i}-\frac{1}{\tau_e} & -i\kappa & 0 & 0 & \cdots & 0 & 0 \\ -i\kappa & -i(\tilde{\omega}+\Delta)+\frac{1}{\tau_i} & -i\kappa & 0 & \cdots & 0 & 0 \\ . & . & . & . & . & . & . \\ . & . & . & . & . & . & . \\ . & . & . & . & . & -i\kappa & -i(\tilde{\omega}+\Delta)+\frac{1}{\tau_i}-\frac{1}{\tau_e} \end{bmatrix} \tilde{\mathbf{a}} - i\omega\begin{bmatrix}\tilde{s}_1\\ \tilde{s}_2\\ .\\ .\\ \tilde{s}_N\end{bmatrix} - i\mu\begin{bmatrix}\tilde{S}_{in}\\ 0\\ .\\ .\\ 0\end{bmatrix} = 0, \tag{32a}$$

$$\tilde{\mathbf{a}} = -i\omega\mathsf{P}^{-1}\tilde{\mathbf{s}} - i\mu\mathsf{P}^{-1}\tilde{\mathbf{s}}_{in}, \tag{32b}$$

where P is the $N\times N$ matrix in Eq. (32a), $\tilde{\mathbf{s}}$ are the spontaneous emission noise sources, and $\tilde{\mathbf{s}}_{in}$ is the input signal. For an input of the form $\tilde{\mathbf{s}}_{in}=[\tilde{S}_{in}\ 0\ 0\ \cdots\ 0]^T$, the amplitude at the Nth resonator is

$$|a_N(\tilde{\omega})|^2=\mu^2|\mathsf{P}_{N,1}^{-1}\tilde{S}_{in}|^2+\omega^2\sum_{j=1}^{N}|\mathsf{P}_{N,j}^{-1}\tilde{s}_j|^2 - \left[\omega\mu(\mathsf{P}_{N,1}^{-1})^*\sum_{j=1}^{N}\mathsf{P}_{N,j}^{-1}\tilde{s}_j\tilde{S}_{in}^*+c.c.\right]. \quad (33)$$

Equation (33) gives the total magnitude of the field at the Nth resonator. We note that the first term on the right side is the signal, the second term is the spontaneous emission, and the last term corresponds to the beating between the input and the spontaneous emission. For strong input powers and weak amplification, the beat noise dominates. We shall proceed to analyze this ideal case where the spontaneous emission signal beat noise is dominant. The other noise term can be dealt with easily in a similar fashion.

The noise current from the beating is given by

$$i_n(\tilde{\omega})=-\eta\omega\mu(\mathsf{P}_{N,1}^{-1})^*\sum_{j=1}^{N}\mathsf{P}_{N,j}^{-1}\tilde{s}_j\tilde{S}_{in}^*+c.c., \quad (34)$$

where η is the responsivity of the detector and accounts for the normalization of a_n. The mean electrical noise power is given by $\langle i_n^2\rangle$, which using the Weiner–Khintchine theorem is

$$\langle i_n^2\rangle=\eta^2\lim_{T\to\infty}\frac{1}{T}\int d\tilde{\omega}2\omega^2\mu^2|\mathsf{P}_{N,1}^{-1}\tilde{S}_{in}|^2\sum_{j,k=1}^{N}\mathsf{P}_{N,j}^{-1}(\mathsf{P}_{N,k}^{-1})^*\tilde{s}_j\tilde{s}_k^* + \omega^2\mu^2 2\,\mathrm{Re}\left[(\mathsf{P}_{N,1}^{-1})^{*2}\tilde{S}_{in}^{*2}\sum_{j,k=1}^{N}\mathsf{P}_{N,j}^{-1}\mathsf{P}_{N,k}^{-1}\tilde{s}_j\tilde{s}_k\right]. \quad (35)$$

Since the spontaneous emission noise is not correlated in amplitude and phase, $\int d\tilde{\omega}\tilde{s}_l^*(\tilde{\omega})\tilde{s}_m(\tilde{\omega})\propto\delta_{l,m}$, where $\delta_{l,m}=0$ for $l\neq m$ and 1 for $l=m$. Therefore, Eq. (35) simplifies to

$$\langle i_n^2\rangle=\eta^2\lim_{T\to\infty}\frac{1}{T}\int d\tilde{\omega}2\omega^2\mu^2|\mathsf{P}_{N,1}^{-1}\tilde{s}_{in}|^2\sum_{j=1}^{N}|\mathsf{P}_{N,j}^{-1}\tilde{s}_j|^2. \quad (36)$$

If we only consider a narrow-band signal and noise contributions within this narrow bandwidth, the integral in the above equation can be approximated by the product of the integrand at $\tilde{\omega}=0$ and the bandwidth $\Delta\tilde{\omega}$. Therefore

$$\langle i_n^2\rangle\approx\eta^2\lim_{T\to\infty}\frac{1}{T}\left[2\omega^2\mu^2|\mathsf{P}_{N,1}^{-1}\tilde{S}_{in}|^2\sum_{j=1}^{N}|\mathsf{P}_{N,j}^{-1}\tilde{s}_j|^2\Delta\tilde{\omega}\right]_{\tilde{\omega}=0} = \omega^2\mu^2|\mathsf{T}_{N,1}\tilde{S}_{in}(0)|^2\sum_{j=1}^{N}|\mathsf{T}_{N,j}|^2\frac{\hbar R_{sp,j}}{2\pi^2V\Omega}\Delta\tilde{\omega}, \quad (37)$$

where we have substituted the result from Eq. (31) and the matrix T was defined in Subsection 3.B.3.

To find the SNR, we first note that the signal is given by

$$\langle i_{in}^2\rangle=\eta^2\mu^4\lim_{T\to\infty}\frac{2\pi}{T}\int d\tilde{\omega}|\mathsf{P}_{N,1}^{-1}\tilde{S}_{in}|^4 \approx\eta^2\mu^4\lim_{T\to\infty}\frac{2\pi}{T}|\mathsf{T}_{N,1}\tilde{S}_{in}(0)|^4\Delta\tilde{\omega}, \quad (38)$$

where the second part of the equation is with the narrow-band approximation. Therefore, if the resonators are identical so that $R_{sp,j}=R_{sp}$, the SNR is

$$\mathrm{SNR}=\frac{4\pi^3V\Omega\mu^2|\mathsf{T}_{N,1}|^2}{\hbar\omega^2R_{sp}\sum_{j=1}^{N}|\mathsf{T}_{N,j}|^2}\cdot\lim_{T\to\infty}\frac{|\tilde{S}_{in}(0)|^2}{T}. \quad (39)$$

$\lim_{T\to\infty}|\tilde{S}_{in}(\tilde{\omega})|^2/T$ is the power spectral density of the input, so the rightmost term in the above equation refers to the input power at ω.

Physically, Eq. (39) states that the beat noise at any frequency at the output is simply the sum of the transmitted magnitudes of spontaneous emission originating from each resonator in the CROW. The key difference between a CROW and a nonresonant amplifier is that the SNR can vary dramatically at different signal frequencies because T can be a strong function of the wavelength. To have an acceptable SNR, the matrix elements, $|\mathsf{T}_{N,j}|^2$, should have a small magnitude. This can be achieved if resonators are not high loss to begin with so that the gain can be kept weak. A reduced pump rate also reduces R_{sp}.

Figure 5 shows the normalized SNR factor, $G=R_{sp0}|\mathsf{T}_{N,1}|^2/R_{sp}\sum_{j=1}^{N}|\mathsf{T}_{N,j}|^2$ as a function of wavelength for various values of τ_g. R_{sp0} is the spontaneous emission rate when $\tau_i=0$ or $\tau_{g0}=\tau_l$. For weak, unsaturated gain, $R_{sp0}/R_{sp}\approx\tau_g/\tau_{g0}$, since both R_{sp} and $1/\tau_g$ vary linearly with the pump rate. τ_l is taken to be a constant at 10^4. As evidenced by the figure, a higher gain leads to a reduction in the SNR. The SNR is also highest at the band-center and lowest at the band edges.

C. Noise Figure

A second parameter that characterizes the performance of an amplifier is the noise figure. The noise figure (NF) is defined as

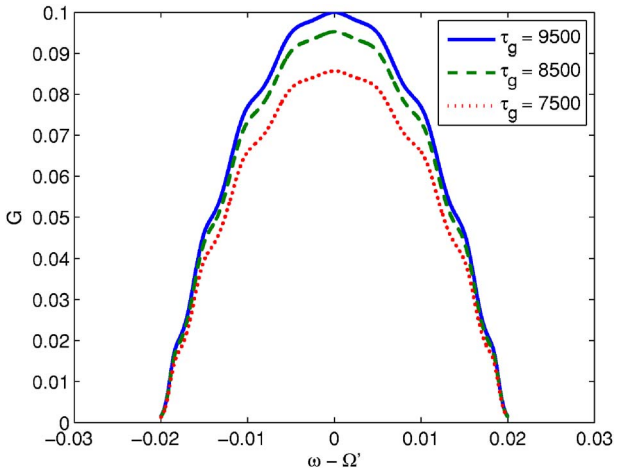

Fig. 5. (Color online) The normalized SNR factor, G, as a function of wavelength at various gain levels. For the calculations, $\tau_l=10^4$, $\kappa=0.01$, $\tau_e=100$, $N=10$.

$$\mathrm{NF} = \frac{\mathrm{SNR}_{in}}{\mathrm{SNR}_{out}}, \tag{40}$$

where SNR_{in} is the SNR at the input of the amplifier and SNR_{out} is the SNR at the output. To determine the NF, we simply need to define our input as $S_{in}=S_{sig}+S_{\delta}$, where S_{sig} is the field amplitude of the signal and S_{δ} is the field amplitude of the noise.

Substituting this form of the input into Eq. (38), and assuming a narrow bandwidth signal, we find

$$\mathrm{SNR}_{in} = \frac{|\tilde{S}_{sig}(0)|^2}{2|\tilde{S}_{\delta}(0)|^2}. \tag{41}$$

At the output, using Eq. (39), we have

$$\mathrm{SNR}_{out} = \frac{4\pi^3 V\Omega\mu^2|\mathsf{T}_{N,1}|^2}{\hbar\omega^2 R_{sp}\sum_{j=1}^{N}|\mathsf{T}_{N,j}|^2}\cdot\lim_{T\to\infty}\frac{|\tilde{S}_{sig}(0)|^2+|\tilde{S}_{\delta}(0)|^2}{T}. \tag{42}$$

Therefore, the noise figure, in the limit $|\tilde{S}_{\delta}(0)|^2 \ll |\tilde{S}_{sig}(0)|^2$, is

$$\mathrm{NF} = \frac{\hbar\omega^2 R_{sp}\sum_{j=1}^{N}|\mathsf{T}_{N,j}|^2}{4\pi^3 V\Omega\mu^2|\mathsf{T}_{N,1}|^2}\cdot\lim_{T\to\infty}\frac{T}{2|\tilde{S}_{\delta}(0)|^2}. \tag{43}$$

In the scenario in which the noise is at the standard quantum limit (i.e., shot noise), S_{δ} is the due to the vacuum fluctuations of the electric field. The quantization of the field gives

$$\hat{S}_{\delta}(t) = \sqrt{\frac{\hbar\omega}{V}}\hat{A}(t), \tag{44}$$

where $\hat{S}(t)$ is now an operator and $\hat{A}(t)$ is the photon annihilation operator [30]. The expectation value is

$$\frac{1}{2}\langle\hat{S}_{\delta}^{\dagger}\hat{S}_{\delta}+\hat{S}_{\delta}\hat{S}_{\delta}^{\dagger}\rangle = \frac{\hbar\omega}{2V}, \tag{45}$$

since the noise arises from the vacuum, $|0\rangle$, photon state. On the other hand, the classical equivalence is

$$\langle S_{\delta}^2\rangle = \lim_{T\to\infty}\frac{2\pi}{T}\int \mathrm{d}\tilde{\omega}|\tilde{S}_{\delta}(\tilde{\omega})|^2 \approx \lim_{T\to\infty}\frac{2\pi}{T}|\tilde{S}_{\delta}(0)|^2\Delta\tilde{\omega}. \tag{46}$$

Therefore, equating Eq. (45) with Eq. (46), we have

$$\lim_{T\to\infty}\frac{|\tilde{S}_{\delta}(0)|^2}{T} = \frac{\hbar\omega}{4\pi V\Delta\tilde{\omega}}. \tag{47}$$

Taking $\Delta\tilde{\omega}=2\kappa$, the bandwidth of a CROW band, and $\omega \approx \Omega$, the noise figure is

$$\mathrm{NF} = \frac{\kappa R_{sp}\sum_{j=1}^{N}|\mathsf{T}_{N,j}|^2}{\pi^2\mu^2|\mathsf{T}_{N,1}|^2}. \tag{48}$$

Figure 6 shows an estimate of the noise figure for a loss-compensated CROW where $1/\tau_i=0$. R_{sp} is given by $R_{sp}=N_2V_{cav}/t_{sp}$, where N_2 is the population density of the excited state of the gain medium, V_{cav} is the active volume of the resonator, and t_{sp} is the spontaneous emission lifetime. Taking $N_2=10^{18}\,\mathrm{cm}^{-3}$, $V_{cav}=10\ \mu\mathrm{m}\times 10\ \mu\mathrm{m}\times 50\ \mathrm{nm}$, and $t_{sp}=1\ \mathrm{ns}$, we compute Eq. (48) at the band-center frequency for various values of inter-resonator coupling coefficients at a fixed input/output coupling constant of $\tau_e=1000$ and $\mu=0.045$. The noise figure depends strongly on the input/output coupling as well as the inter-resonator coupling. Nonetheless, using these rough estimates, we see that loss-compensated CROWs of the order of tens of resonators long can maintain noise figures of less than five.

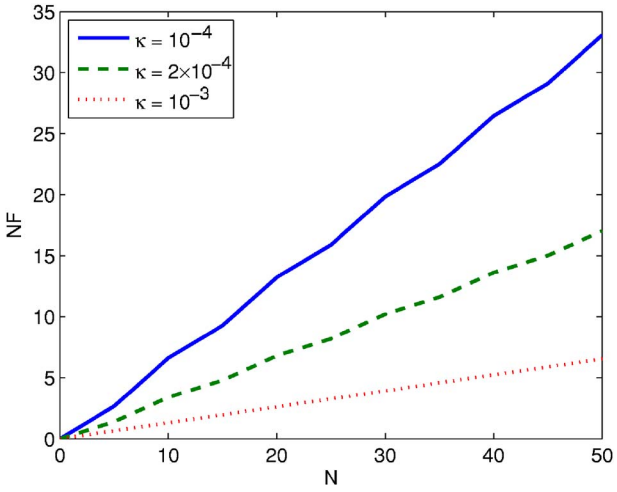

Fig. 6. (Color online) The NF as a function of the number of resonators (N) in an active CROW at the band-center frequency where the losses are exactly compensated. The parameters for the calculations are in the text.

5. DISCUSSION

We have elucidated the effect of the boundary conditions on the net gain in a CROW and the spontaneous emission on the SNR. Our results imply that the transmission spectra, gain/loss, and noise of CROWs depend significantly on the exact configuration of the CROWs and how they are excited. The dispersion relation of an infinite structure, in the presence of gain (or loss), does not necessarily model a periodic structure of finite length regardless of the number of periods that constitute the device. While the real part of the phase accumulated in a finite CROW can be similar to an infinite structure, the imaginary part of the phase (loss/gain) can differ significantly.

Our results show that gain/loss enhancement in CROWs does not strictly depend on $\bar{v}_g$, but can instead be understood as the combined effect of the gain/loss of the individual cavities and the resonance due to the finite length of the structure. Since the effective reflectivity of a semi-infinite CROW is highest at the band-edges [24], the "large" resonator set up in the direction of periodicity consisting of all the cavities in the CROW is lowest loss for the band-edge or low $\bar{v}_g$ modes. In the same way that transmission spectrum ripples can be minimized by modifying only the input/output coupling coefficients in a CROW [24], the gain (and loss) can also be controlled. The dependence of optical loss on the structural termination has been observed in photonic crystals [31], and the de-

pendence of the laser frequencies and cleaved facets have been analyzed in distributed feedback lasers [32]. The effect of the termination on the optical properties of periodic structures should be explored in greater detail.

Our calculations of active CROWs with an input at the first resonator and output show that the frequencies near the band-center have the highest SNR. Fortuitously, the band-center is also the region of lowest group velocity dispersion, and its dispersive properties are the most robust to disorder in the coupling constants [33,34]. Naturally then, the most ideal frequencies for the propagation of optical signals with small $\bar{v}_g$ should be those near the CROW band-center. In contrast to other types of periodic structures, such as gratings and photonic crystals, the small group velocities at the band-edges are accompanied by a large group velocity dispersion. The value of the SNR is also unclear at those frequencies.

Although we have not formulated a complete picture of amplification in CROWs, which would require additional equations to describe the carrier densities and a quantum mechanical treatment of the transition rates (to derive the gain/loss, noise), we briefly note the impact of $\bar{v}_g$ on the induced optical transition rates and the gain. For a simple two-level atom model, the induced transition rate, W_i, is proportional to the optical intensity [30], which is higher for reduced group velocities. To show this, we observe that, for a monochromatic wave in a homogeneous medium, its intensity is

$$I(\omega) = \frac{cn_{ph}\hbar\omega}{nV}, \tag{49}$$

where n_{ph} is then the number of photons in the mode oscillating at ω, V is the modal volume, and n is the effective index of the medium. However,

$$n_{ph} = \rho(\omega)\mathrm{d}\omega = \rho(K)\mathrm{d}K, \tag{50}$$

where $\rho(\omega)$ is the photon density of states in frequency and $\rho(K)$ is the density of states in wavenumber. Because $v_g = \mathrm{d}\omega/\mathrm{d}K$ and $\rho(K) = N\Lambda/2\pi$ [34], substituting into Eq. (50), we have

$$n_{ph} = \frac{N\Lambda}{2\pi}\frac{\delta\omega}{v_g(\omega)}. \tag{51}$$

Thus, a small group velocity leads to a higher stimulated emission rate. However, the optical gain does not strictly depend on W_i. Rather, the optical amplification rate is the fractional increase in the intensity of a wave per unit time, i.e., $\dot{I}/I = \dot{n}_{ph}/n_{ph}$ [30]. Since $\dot{n}_{ph}$ is also proportional to W_i, the $1/v_g$ contribution cancels. This implies that although W_i scales with $1/v_g$, the gain does not necessarily. In practice, the gain may also be lower for higher intensity modes because of saturation. Thus, in CROW lasers, the lowest v_g or band-edge modes need not be the first to oscillate nor does it have to oscillate at all.

6. CONCLUSION

In summary, we have presented a derivation of the time domain tight-binding equations describing the modes and wave propagation in CROWs. Only in the limit of weak coupling and weak gain does the tight-binding equation resemble the simple coupled oscillator equations commonly found in literature. Using this formalism, we find that the termination and excitation of a CROW has a profound impact on the net gain of an optical wave inside the structure. A finite CROW can have significantly different amplification and loss properties compared to an infinitely long chain of resonators. Finally, we have derived the SNR and the noise figure of amplifying CROWs using the tight-binding approach.

ACKNOWLEDGMENTS

J. K. S. Poon thanks Philip Chak and Lin Zhu for fruitful discussions. She is grateful for the support of the Natural Sciences and Engineering Research Council of Canada. The support of the Defense Advanced Research Projects Agency (Slow Light Project) and National Science Foundation (award 0438038) are gratefully acknowledged.

REFERENCES

1. A. Yariv, Y. Xu, R. K. Lee, and A. Scherer, "Coupled-resonator optical waveguide: a proposal and analysis," Opt. Lett. **24**, 711–713 (1999).
2. N. Stefanou and A. Modinos, "Impurity bands in photonic insulators," Phys. Rev. B **57**, 12,127–12,133 (1998).
3. J. K. S. Poon, L. Zhu, G. A. DeRose, and A. Yariv, "Polymer microring coupled-resonator optical waveguides," J. Lightwave Technol. **24**, 1843–1849 (2006).
4. M. Bayindir, S. Tanriseven, and E. Ozbay, "Propagation of light through localized coupled-cavity modes in one-dimensional photonic band-gap structures," Appl. Phys. A **72**, 117–119 (2001).
5. S. Olivier, C. Smith, M. Rattier, H. Benisty, C. Weisbuch, T. Krauss, R. Houdre, and U. Osterle, "Miniband transmission in a photonic crystal waveguide coupled-resonator optical waveguide," Opt. Lett. **26**, 1019–1051 (2001).
6. S. Lan, S. Nishikawa, H. Ishikawa, and O. Wada, "Engineering photonic crystal impurity bands for waveguides, all-optical switches and optical delay lines," IEICE Trans. Electron. **E85C**, 181–189 (2002).
7. B. E. Little, S. T. Chu, P. P. Absil, J. V. Hryniewicz, F. G. Johnson, F. Seiferth, D. Gill, V. Van, O. King, and M. Trakalo, "Very high-order microring resonator filters for WDM applications," IEEE Photon. Technol. Lett. **16**, 2263–2265 (2004).
8. J. K. S. Poon, L. Zhu, G. A. DeRose, and A. Yariv, "Transmission and group delay in microring coupled-resonator optical waveguides," Opt. Lett. **31**, 456–458 (2006).
9. F. Xia, L. Sekaric, and Y. Vlasov, "Ultracompact optical buffers on a silicon chip," Nat. Photonics **1**, 65–71 (2007).
10. J. K. S. Poon, J. Scheuer, Y. Xu, and A. Yariv, "Designing coupled-resonator optical waveguide delay lines," J. Opt. Soc. Am. B **21**, 1665–1673 (2004).
11. J. K. S. Poon, L. Zhu, G. A. DeRose, J. M. Choi, and A. Yariv, "Active coupled-resonator optical waveguides. II. Current injection InP–InGaAsP Fabry–Perot resonator arrays," J. Opt. Soc. Am. B **24**, 2389–2393 (2007).
12. H. A. Haus, *Waves and Fields in Optoelectronics* (Prentice-Hall, 1984).
13. B. E. Little, S. T. Chu, H. A. Haus, J. Foresi, and J.-P. Laine, "Microring resonator channel dropping filter," J. Lightwave Technol. **15**, 998–1005 (1997).
14. S. S. Wang and H. G. Winful, "Dynamics of phase-locked semiconductor laser arrays," Appl. Phys. Lett. **52**, 1774–1776 (1988).
15. R. K. Chang and A. J. Campillo, *Optical Processes in Microcavities* (World Scientific, 1996).

16. C. H. Henry, "Theory of spontaneous emission noise in open resonators and its application to lasers and optical amplifiers," J. Lightwave Technol. **4**, 288–297 (1986).
17. J. K. S. Poon, J. Scheuer, S. Mookherjea, G. T. Paloczi, Y. Huang, and A. Yariv, "Matrix analysis of microring coupled-resonator optical waveguides," Opt. Express **12**, 90–103 (2004).
18. J. K. S. Poon, P. Chak, J. M. Choi, and A. Yariv, "Slowing light with Fabry–Perot resonator arrays," J. Opt. Soc. Am. B, submitted for publication.
19. S. Mookherjea, "Using gain to tune the dispersion relation of coupled-resonator optical waveguides," IEEE Photon. Technol. Lett. **18**, 715–717 (2006).
20. J. P. Dowling, M. Scalora, M. J. Bloemer, and C. M. Bowden, "The photonic band-edge laser—a new approach to gain enhancement," Appl. Phys. Lett. **75**, 1896–1899 (1994).
21. S. Nojima, "Enhancement of optical gain in two-dimensional photonic crystals with active lattice points," Jpn. J. Appl. Phys., Part 2 **37**, L565–L567 (1998).
22. L. Florescu, K. Busch, and S. John, "Semiclassical theory of lasing in photonic crystals," J. Opt. Soc. Am. B **19**, 2215–2223 (2002).
23. A. Yariv, *Optical Electronics in Modern Communications*, 5th ed. (Oxford University Press, 1997).
24. P. Chak and J. Sipe, "Minimizing finite-size effects in artificial resonance tunneling structures," Opt. Lett. **13**, 2568–2570 (2006).
25. W. C. Yueh, "Explicit inverses of several tridiagonal matrices," Appl. Math. E-Notes **6**, 74–83 (2006).
26. U. Peschel, A. L. Reynolds, B. Arredondo, F. Lederer, P. J. Roberts, T. F. Krauss, and P. J. I. de Maagt, "Transmission and reflection analysis of functional coupled cavity components," IEEE J. Quantum Electron. **38**, 830–836 (2002).
27. T. Mukai and Y. Yamamoto, "Noise in an AlGaAs semiconductor-laser amplifier," IEEE J. Quantum Electron. **18**, 564–575 (1982).
28. N. A. Olsson, "Heterodyne gan and noise measurement of a 1.5 μm resonasnt semiconductor-laser amplifier," IEEE J. Quantum Electron. **22**, 671–676 (1986).
29. R. J. Lang and A. Yariv, "Semiclassical theory of noise in multielement semiconductor lasers," IEEE J. Quantum Electron. **22**, 436–449 (1986).
30. A. Yariv, *Quantum Electronics*, 3rd ed. (Wiley, 1989).
31. Y. A. Vlasov and S. J. McNab, "Coupling into the slowlight mode in slab-type photonic crystal waveguides," Opt. Lett. **31**, 50–52 (2006).
32. G. P. Agrawal and N. K. Dutta, *Long-Wavelength Semiconductor Lasers* (Van Nostrand Reinhold Company, 1986).
33. S. Mookherjea, "Spectral characteristics of coupled resonators," J. Opt. Soc. Am. B **23**, 1137–1145 (2006).
34. S. Mookherjea and A. Oh, "Effect of disorder on slow light velocity in optical slow-wave structures," Opt. Lett. **32**, 289–291 (2007).